CHAPTER 4

Flow of Fluids through Granular Beds and Packed Columns

4.1. INTRODUCTION

The flow of fluids through beds composed of stationary granular particles is a frequent occurrence in the chemical industry and therefore expressions are needed to predict pressure drop across beds due to the resistance caused by the presence of the particles. For example, in fixed bed catalytic reactors, such as SO_2-SO_3 converters, and drying columns containing silica gel or molecular sieves, gases are passed through a bed of particles. In the case of gas absorption into a liquid, the gas flows upwards against a falling liquid stream, the fluids being contained in a vertical column packed with shaped particles. In the filtration of a suspension, liquid flows at a relatively low velocity through the spaces between the particles which have been retained by the filter medium and, as a result of the continuous deposition of solids, the resistance to flow increases progressively throughout the operation. Furthermore, deep bed filtration is used on a very large scale in water treatment, for example, where the quantity of solids to be removed is small. In all these instances it is necessary to estimate the size of the equipment required, and design expressions are required for the drop in pressure for a fluid flowing through a packing, either alone or as a two-phase system. The corresponding expressions for fluidised beds are discussed in Chapter 6. The drop in pressure for flow through a bed of small particles provides a convenient method for obtaining a measure of the external surface area of a powder, for example cement or pigment.

The flow of either a single phase through a bed of particles or the more complex flow of two fluid phases is approached by using the concepts developed in Volume 1 for the flow of an incompressible fluid through regular pipes or ducts. It is found, however, that the problem is not in practice capable of complete analytical solution and the use of experimental data obtained for a variety of different systems is essential. Later in the chapter some aspects of the design of industrial packed columns involving countercurrent flow of liquids and gases are described.

4.2. FLOW OF A SINGLE FLUID THROUGH A GRANULAR BED

4.2.1. Darcy's law and permeability

The first experimental work on the subject was carried out by DARCY[1] in 1830 in Dijon when he examined the rate of flow of water from the local fountains through beds of

sand of various thicknesses. It was shown that the average velocity, as measured over the whole area of the bed, was directly proportional to the driving pressure and inversely proportional to the thickness of the bed. This relation, often termed Darcy's law, has subsequently been confirmed by a number of workers and can be written as follows:

$$u_c = K\frac{(-\Delta P)}{l} \tag{4.1}$$

where $-\Delta P$ is the pressure drop across the bed,
l is the thickness of the bed,
u_c is the average velocity of flow of the fluid, defined as $(1/A)(\mathrm{d}V/\mathrm{dt})$,
A is the total cross sectional area of the bed,
V is the volume of fluid flowing in time t, and
K is a constant depending on the physical properties of the bed and fluid.

The linear relation between the rate of flow and the pressure difference leads one to suppose that the flow was streamline, as discussed in Volume 1, Chapter 3. This would be expected because the Reynolds number for the flow through the pore spaces in a granular material is low, since both the velocity of the fluid and the width of the channels are normally small. The resistance to flow then arises mainly from viscous drag. Equation 4.1 can then be expressed as:

$$u_c = \frac{K(-\Delta P)}{l} = B\frac{(-\Delta P)}{\mu l} \tag{4.2}$$

where μ is the viscosity of the fluid and B is termed the permeability coefficient for the bed, and depends only on the properties of the bed.

The value of the permeability coefficient is frequently used to give an indication of the ease with which a fluid will flow through a bed of particles or a filter medium. Some values of B for various packings, taken from EISENKLAM[2], are shown in Table 4.1, and it can be seen that B can vary over a wide range of values. It should be noted that these values of B apply only to the laminar flow regime.

4.2.2. Specific surface and voidage

The general structure of a bed of particles can often be characterised by the specific surface area of the bed S_B and the fractional voidage of the bed e.

S_B is the surface area presented to the fluid per unit volume of bed when the particles are packed in a bed. Its units are $(\text{length})^{-1}$.

e is the fraction of the volume of the bed not occupied by solid material and is termed the fractional voidage, voidage, or porosity. It is dimensionless. Thus the fractional volume of the bed occupied by solid material is $(1 - e)$.

S is the specific surface area of the particles and is the surface area of a particle divided by its volume. Its units are again $(\text{length})^{-1}$. For a sphere, for example:

$$S = \frac{\pi d^2}{\pi(d^3/6)} = \frac{6}{d} \tag{4.3}$$

Table 4.1. Properties of beds of some regular-shaped materials[2]

No.	Solid constituents: Description	Specific surface area S (m^2/m^3)	Porous mass: Fractional voidage, e (−)	Porous mass: Permeability coefficient B (m^2)
	Spheres			
1	0.794 mm diam. ($\frac{1}{32}$ in.)	7600	0.393	6.2×10^{-10}
2	1.588 mm diam. ($\frac{1}{16}$ in.)	3759	0.405	2.8×10^{-9}
3	3.175 mm diam. ($\frac{1}{8}$ in.)	1895	0.393	9.4×10^{-9}
4	6.35 mm diam. ($\frac{1}{4}$ in.)	948	0.405	4.9×10^{-8}
5	7.94 mm diam. ($\frac{5}{16}$ in.)	756	0.416	9.4×10^{-8}
	Cubes			
6	3.175 mm ($\frac{1}{8}$ in.)	1860	0.190	4.6×10^{-10}
7	3.175 mm ($\frac{1}{8}$ in.)	1860	0.425	1.5×10^{-8}
8	6.35 mm ($\frac{1}{4}$ in.)	1078	0.318	1.4×10^{-8}
9	6.35 mm ($\frac{1}{4}$ in.)	1078	0.455	6.9×10^{-8}
	Hexagonal prisms			
10	4.76 mm × 4.76 mm thick ($\frac{3}{16}$ in. × $\frac{3}{16}$ in.)	1262	0.355	1.3×10^{-8}
11	4.76 mm × 4.76 mm thick ($\frac{3}{16}$ in. × $\frac{3}{16}$ in.)	1262	0.472	5.9×10^{-8}
	Triangular pyramids			
12	6.35 mm length × 2.87 mm ht. ($\frac{1}{4}$ in. × 0.113 in.)	2410	0.361	6.0×10^{-9}
13	6.35 mm length × 2.87 mm ht. ($\frac{1}{4}$ in. × 0.113 in.)	2410	0.518	1.9×10^{-8}
	Cylinders			
14	3.175 mm × 3.175 mm diam. ($\frac{1}{8}$ in. × $\frac{1}{8}$ in.)	1840	0.401	1.1×10^{-8}
15	3.175 mm × 6.35 mm diam. ($\frac{1}{8}$ in. × $\frac{1}{4}$ in.)	1585	0.397	1.2×10^{-8}
16	6.35 mm × 6.35 mm diam. ($\frac{1}{4}$ in. × $\frac{1}{4}$ in.)	945	0.410	4.6×10^{-8}
	Plates			
17	6.35 mm × 6.35 mm × 0.794 mm ($\frac{1}{4}$in. × $\frac{1}{4}$in. × $\frac{1}{32}$ in.)	3033	0.410	5.0×10^{-9}
18	6.35 mm × 6.35 mm × 1.59 mm ($\frac{1}{4}$in. × $\frac{1}{4}$in. × $\frac{1}{16}$ in.)	1984	0.409	1.1×10^{-8}
	Discs			
19	3.175 mm diam. × 1.59 mm ($\frac{1}{8}$ in. × $\frac{1}{16}$ in.)	2540	0.398	6.3×10^{-9}
	Porcelain Berl saddles			
20	6 mm (0.236 in.)	2450	0.685	9.8×10^{-8}
21	6 mm (0.236 in.)	2450	0.750	1.73×10^{-7}
22	6 mm (0.236 in.)	2450	0.790	2.94×10^{-7}
23	6 mm (0.236 in.)	2450	0.832	3.94×10^{-7}
24	Lessing rings (6 mm)	5950	0.870	1.71×10^{-7}
25	Lessing rings (6 mm)	5950	0.889	2.79×10^{-7}

It can be seen that S and S_B are not equal due to the voidage which is present when the particles are packed into a bed. If point contact occurs between particles so that only a very small fraction of surface area is lost by overlapping, then:

$$S_B = S(1 - e) \tag{4.4}$$

Some values of S and e for different beds of particles are listed in Table 4.1. Values of e much higher than those shown in Table 4.1, sometimes up to about 0.95, are possible in beds of fibres[3] and some ring packings. For a given shape of particle, S increases as the particle size is reduced, as shown in Table 4.1.

As e is increased, flow through the bed becomes easier and so the permeability coefficient B increases; a relation between B, e, and S is developed in a later section of this chapter. If the particles are randomly packed, then e should be approximately constant throughout the bed and the resistance to flow the same in all directions. Often near containing walls, e is higher, and corrections for this should be made if the particle size is a significant fraction of the size of the containing vessel. This correction is discussed in more detail later.

4.2.3. General expressions for flow through beds in terms of Carman–Kozeny equations

Streamline flow — Carman–Kozeny equation

Many attempts have been made to obtain general expressions for pressure drop and mean velocity for flow through packings in terms of voidage and specific surface, as these quantities are often known or can be measured. Alternatively, measurements of the pressure drop, velocity, and voidage provide a convenient way of measuring the surface area of some particulate materials, as described later.

The analogy between streamline flow through a tube and streamline flow through the pores in a bed of particles is a useful starting point for deriving a general expression.

From Volume 1, Chapter 3, the equation for streamline flow through a circular tube is:

$$u = \frac{d_t^2}{32\mu}\frac{(-\Delta P)}{l_t} \tag{4.5}$$

where: μ is the viscosity of the fluid,
u is the mean velocity of the fluid,
d_t is the diameter of the tube, and
l_t is the length of the tube.

If the free space in the bed is assumed to consist of a series of tortuous channels, equation 4.5 may be rewritten for flow through a bed as:

$$u_1 = \frac{d_m'^2}{K'\mu}\frac{(-\Delta P)}{l'} \tag{4.6}$$

where: d_m' is some equivalent diameter of the pore channels,
K' is a dimensionless constant whose value depends on the structure of the bed,
l' is the length of channel, and
u_1 is the average velocity through the pore channels.

It should be noted that u_1 and l' in equation 4.6 now represent conditions in the pores and are not the same as u_c and l in equations 4.1 and 4.2. However, it is a reasonable

assumption that l' is directly proportional to l. DUPUIT[4] related u_c and u_1 by the following argument.

In a cube of side X, the volume of free space is eX^3 so that the mean cross-sectional area for flow is the free volume divided by the height, or eX^2. The volume flowrate through this cube is u_cX^2, so that the average linear velocity through the pores, u_1, is given by:

$$u_1 = \frac{u_cX^2}{eX^2} = \frac{u_c}{e} \tag{4.7}$$

Although equation 4.7 is reasonably true for random packings, it does not apply to all regular packings. Thus with a bed of spheres arranged in cubic packing, $e = 0.476$, but the fractional free area varies continuously, from 0.215 in a plane across the diameters to 1.0 between successive layers.

For equation 4.6 to be generally useful, an expression is needed for d'_m, the equivalent diameter of the pore space. KOZENY[5,6] proposed that d'_m may be taken as:

$$d'_m = \frac{e}{S_B} = \frac{e}{S(1-e)} \tag{4.8}$$

where:

$$\frac{e}{S_B} = \frac{\text{volume of voids filled with fluid}}{\text{wetted surface area of the bed}}$$

$$= \frac{\text{cross-sectional area normal to flow}}{\text{wetted perimeter}}$$

The hydraulic mean diameter for such a flow passage has been shown in Volume 1, Chapter 3 to be:

$$4\left(\frac{\text{cross-sectional area}}{\text{wetted perimeter}}\right)$$

It is then seen that:

$$\frac{e}{S_B} = \tfrac{1}{4}\ \text{(hydraulic mean diameter)}$$

Then taking $u_1 = u_c/e$ and $l' \propto l$, equation 4.6 becomes:

$$u_c = \frac{1}{K''}\frac{e^3}{S_B^2}\frac{1}{\mu}\frac{(-\Delta P)}{l}$$

$$= \frac{1}{K''}\frac{e^3}{S^2(1-e)^2}\frac{1}{\mu}\frac{(-\Delta P)}{l} \tag{4.9}$$

K'' is generally known as Kozeny's constant and a commonly accepted value for K'' is 5. As will be shown later, however, K'' is dependent on porosity, particle shape, and other factors. Comparison with equation 4.2 shows that B the permeability coefficient is given by:

$$B = \frac{1}{K''}\frac{e^3}{S^2(1-e)^2} \tag{4.10}$$

Inserting a value of 5 for K'' in equation 4.9:

$$u_c = \frac{1}{5}\frac{e^3}{(1-e)^2}\frac{-\Delta P}{S^2\mu l} \tag{4.11}$$

For spheres: $S = 6/d$ and: (equation 4.3)

$$u_c = \frac{1}{180}\frac{e^3}{(1-e)^2}\frac{-\Delta P d^2}{\mu l} \tag{4.12}$$

$$= 0.0055\frac{e^3}{(1-e)^2}\frac{-\Delta P d^2}{\mu l} \tag{4.12a}$$

For non-spherical particles, the Sauter mean diameter d_s should be used in place of d. This is given in Chapter 1, equation 1.15.

Streamline and turbulent flow

Equation 4.9 applies to streamline flow conditions, though CARMAN[7] and others have extended the analogy with pipe flow to cover both streamline and turbulent flow conditions through packed beds. In this treatment a modified friction factor $R_1/\rho u_1^2$ is plotted against a modified Reynolds number Re_1. This is analogous to plotting $R/\rho u^2$ against Re for flow through a pipe as in Volume 1, Chapter 3.

The modified Reynolds number Re_1 is obtained by taking the same velocity and characteristic linear dimension d'_m as were used in deriving equation 4.9. Thus:

$$Re_1 = \frac{u_c}{e}\frac{e}{S(1-e)}\frac{\rho}{\mu}$$

$$= \frac{u_c\rho}{S(1-e)\mu} \tag{4.13}$$

The friction factor, which is plotted against the modified Reynolds number, is $R_1/\rho u_1^2$, where R_1 is the component of the drag force per unit area of particle surface in the direction of motion. R_1 can be related to the properties of the bed and pressure gradient as follows. Considering the forces acting on the fluid in a bed of unit cross-sectional area and thickness l, the volume of particles in the bed is $l(1-e)$ and therefore the total surface is $Sl(1-e)$. Thus the resistance force is $R_1 Sl(1-e)$. This force on the fluid must be equal to that produced by a pressure difference of ΔP across the bed. Then, since the free cross-section of fluid is equal to e:

$$(-\Delta P)e = R_1 Sl(1-e)$$

and

$$R_1 = \frac{e}{S(1-e)}\frac{(-\Delta P)}{l} \tag{4.14}$$

Thus

$$\frac{R_1}{\rho u_1^2} = \frac{e^3}{S(1-e)}\frac{(-\Delta P)}{l}\frac{1}{\rho u_c^2} \tag{4.15}$$

Carman found that when $R_1/\rho u_1^2$ was plotted against Re_1 using logarithmic coordinates, his data for the flow through randomly packed beds of solid particles could be correlated approximately by a single curve (curve A, Figure 4.1), whose general equation is:

$$\frac{R_1}{\rho u_1^2} = 5Re_1^{-1} + 0.4Re_1^{-0.1} \tag{4.16}$$

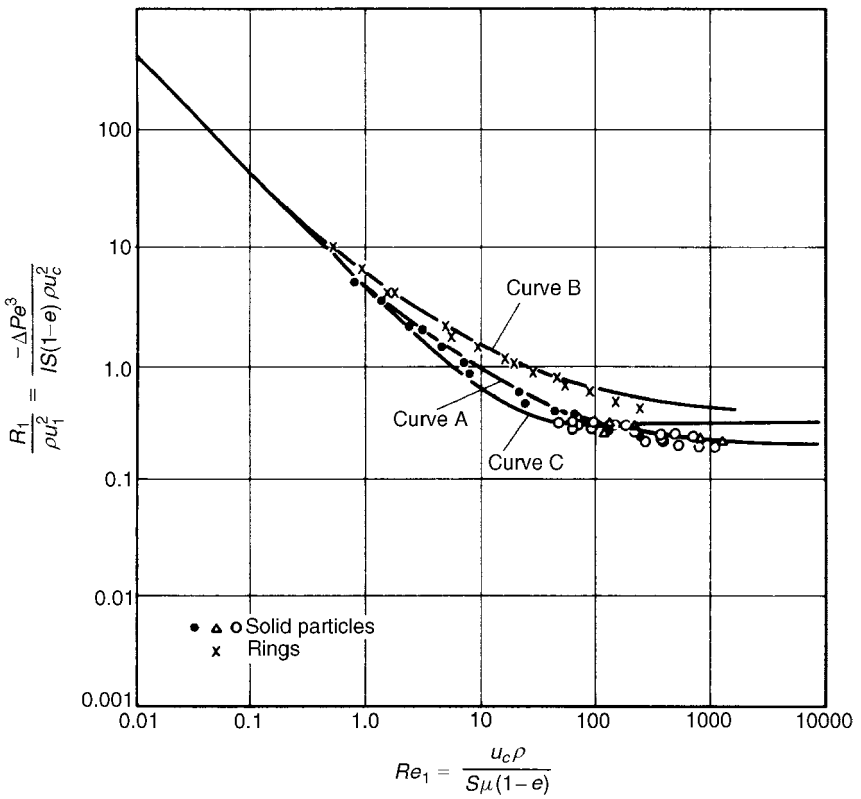

Figure 4.1. Carman's graph of $R_1/\rho u_1^2$ against Re_1

The form of equation 4.16 is similar to that of equation 4.17 proposed by FORCHHEIMER[8] who suggested that the resistance to flow should be considered in two parts: that due to the viscous drag at the surface of the particles, and that due to loss in turbulent eddies and at the sudden changes in the cross-section of the channels. Thus:

$$(-\Delta P) = \alpha u_c + \alpha' u_c^{n'} \tag{4.17}$$

The first term in this equation will predominate at low rates of flow where the losses are mainly attributable to skin friction, and the second term will become significant at high

flowrates and in very thin beds where the enlargement and contraction losses become very important. At very high flowrates the effects of viscous forces are negligible.

From equation 4.16 it can be seen that for values of Re_1 less than about 2, the second term is small and, approximately:

$$\frac{R_1}{\rho u_1^2} = 5Re_1^{-1} \tag{4.18}$$

Equation 4.18 can be obtained from equation 4.11 by substituting for $-\Delta P/l$ from equation 4.15. This gives:

$$u_c = \frac{1}{5}\left(\frac{1}{1-e}\right)\left(\frac{\rho u_c^2}{S\mu}\right)\left(\frac{R_1}{\rho u_1^2}\right)$$

Thus:

$$\frac{R_1}{\rho u_1^2} = 5\left(\frac{S(1-e)\mu}{u_c\rho}\right)$$

$$= 5Re_1^{-1} \qquad \text{(from equation 4.13)}$$

As the value of Re_1 increases from about 2 to 100, the second term in equation 4.16 becomes more significant and the slope of the plot gradually changes from -1.0 to about $-\frac{1}{4}$. Above Re_1 of 100 the plot is approximately linear. The change from complete streamline flow to complete turbulent flow is very gradual because flow conditions are not the same in all the pores. Thus, the flow starts to become turbulent in the larger pores, and subsequently in successively smaller pores as the value of Re_1 increases. It is probable that the flow never becomes completely turbulent since some of the passages may be so small that streamline conditions prevail even at high flowrates.

Rings, which as described later are often used in industrial packed columns, tend to deviate from the generalised curve A on Figure 4.1 particularly at high values of Re_1.

SAWISTOWSKI[9] compared the results obtained for flow of fluids through beds of hollow packings (discussed later) and has noted that equation 4.16 gives a consistently low result for these materials. He proposed:

$$\frac{R_1}{\rho u_1^2} = 5Re_1^{-1} + Re_1^{-0.1} \tag{4.19}$$

This equation is plotted as curve B in Figure 4.1.

For flow through ring packings which as described later are often used in industrial packed columns, ERGUN[10] obtained a good semi-empirical correlation for pressure drop as follows:

$$\frac{-\Delta P}{l} = 150\frac{(1-e)^2}{e^3}\frac{\mu u_c}{d^2} + 1.75\frac{(1-e)}{e^3}\frac{\rho u_c^2}{d} \tag{4.20}$$

Writing $d = 6/S$ (from equation 4.3):

$$\frac{-\Delta P}{Sl\rho u_c^2}\frac{e^3}{1-e} = 4.17\frac{\mu S(1-e)}{\rho u_c} + 0.29$$

or:

$$\frac{R_1}{\rho u_1^2} = 4.17Re_1^{-1} + 0.29 \tag{4.21}$$

This equation is plotted as curve C in Figure 4.1. The form of equation 4.21 is somewhat similar to that of equations 4.16 and 4.17, in that the first term represents viscous losses which are most significant at low velocities and the second term represents kinetic energy losses which become more significant at high velocities. The equation is thus applicable over a wide range of velocities and was found by Ergun to correlate experimental data well for values of $Re_1/(1-e)$ from 1 to over 2000.

The form of the above equations suggests that the only properties of the bed on which the pressure gradient depends are its specific surface S (or particle size d) and its voidage e. However, the structure of the bed depends additionally on the particle size distribution, the particle shape and the way in which the bed has been formed; in addition both the walls of the container and the nature of the bed support can considerably affect the way the particles pack. It would be expected, therefore, that experimentally determined values of pressure gradient would show a considerable scatter relative to the values predicted by the equations. The importance of some of these factors is discussed in the next section.

Furthermore, the rheology of the fluid is important in determining how it flows through a packed bed. Only Newtonian fluid behaviour has been considered hitherto. For non-Newtonian fluids, the effect of continual changes in the shape and cross-section of the flow passages may be considerable and no simple relation may exist between pressure gradient and flowrate. This problem has been the subject of extensive studies by several workers including Kemblowski *et al.*[11].

In some applications, there may be simultaneous flow of two immiscible liquids, or of a liquid and a gas. In general, one of the liquids (or the liquid in the case of liquid–gas systems) will preferentially wet the particles and flow as a continuous film over the surface of the particles, while the other phase flows through the remaining free space. The problem is complex and the exact nature of the flow depends on the physical properties of the two phases, including their surface tensions. An analysis has been made by several workers including Botset[12] and Glaser and Litt[13].

Dependence of K'' on bed structure

Tortuosity. Although it was implied in the derivation of equation 4.9 that a single value of the Kozeny constant K'' applied to all packed beds, in practice this assumption does not hold.

Carman[7] has shown that:

$$K'' = \left(\frac{l'}{l}\right)^2 \times K_0 \tag{4.22}$$

where (l'/l) is the tortuosity and is a measure of the fluid path length through the bed compared with the actual depth of the bed,

K_0 is a factor which depends on the shape of the cross-section of a channel through which fluid is passing.

For streamline fluid flow through a circular pipe where Poiseuille's equation applies (given in Volume 1, Chapter 3), K_0 is equal to 2.0, and for streamline flow through a rectangle where the ratio of the lengths of the sides is 10 : 1, $K_0 = 2.65$. Carman[14] has listed values of K_0 for other cross-sections. From equation 4.22 it can be seen that if, say,

K_0 were constant, then K'' would increase with increase in tortuosity. The reason for K'' being near to 5.0 for many different beds is probably that changes in tortuosity from one bed to another have been compensated by changes in K_0 in the opposite direction.

Wall effect. In a packed bed, the particles will not pack as closely in the region near the wall as in the centre of the bed, so that the actual resistance to flow in a bed of small diameter is less than it would be in an infinite container for the same flowrate per unit area of bed cross-section. A correction factor f_w for this effect has been determined experimentally by COULSON[15]. This takes the form:

$$f_w = \left(1 + \tfrac{1}{2}\frac{S_c}{S}\right)^2 \tag{4.23}$$

where S_c is the surface of the container per unit volume of bed.

Equation 4.9 then becomes:

$$u_c = \frac{1}{K''}\frac{e^3}{S^2(1-e)^2}\frac{1}{\mu}\frac{(-\Delta P)}{l}f_w \tag{4.24}$$

The values of K'' shown on Figure 4.2 apply to equation 4.24.

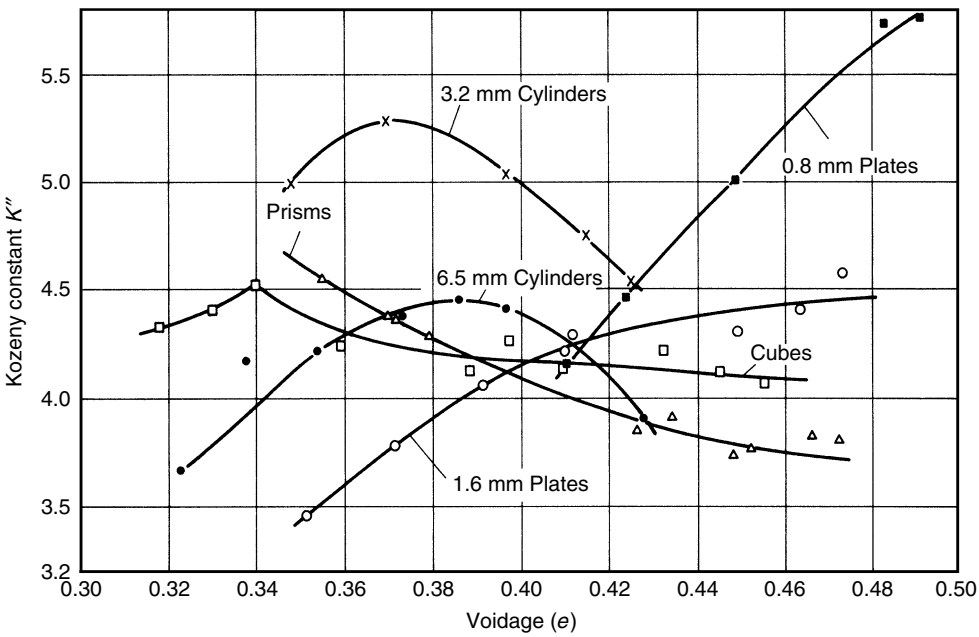

Figure 4.2. Variation of Kozeny's constant K'' with voidage for various shapes

Non-spherical particles. COULSON[15] and WYLLIE and GREGORY[16] have each determined values of K'' for particles of many different sizes and shapes, including prisms, cubes, and plates. Some of these values for K'' are shown in Figure 4.2 where it is seen that they lie

between 3 and 6 with the extreme values only occurring with thin plates. This variation of K'' with plates probably arises, not only from the fact that area contact is obtained between the particles, but also because the plates tend to give greater tortuosities. For normal granular materials KIHN[17] and PIRIE[18] have found that K'' is reasonably constant and does not vary so widely as the K'' values for extreme shapes in Figure 4.2.

Spherical particles. Equation 4.24 has been tested with spherical particles over a wide range of sizes and K'' has been found to be about 4.8 ± 0.3[15,19].

For beds composed of spheres of mixed sizes the porosity of the packing can change very rapidly if the smaller spheres are able to fill the pores between the larger ones. Thus COULSON[15] found that, with a mixture of spheres of size ratio 2 : 1, a bed behaves much in accordance with equation 4.19 but, if the size ratio is 5 : 1 and the smaller particles form less than 30 per cent by volume of the larger ones, then K'' falls very rapidly, emphasising that only for uniform sized particles can bed behaviour be predicted with confidence.

Beds with high voidage. Spheres and particles which are approximately isometric do not pack to give beds with voidages in excess of about 0.6. With fibres and some ring packings, however, values of e near unity can be obtained and for these high values K'' rises rapidly. Some values are given in Table 4.2.

Table 4.2. Experimental values of K'' for beds of high porosity

Voidage e	Experimental value of K''		
	BRINKMAN[3]	DAVIES[21]	Silk fibres LORD[20]
0.5	5.5		
0.6	4.3		
0.8	5.4	6.7	5.35
0.9	8.8	9.7	6.8
0.95	15.2	15.3	9.2
0.98	32.8	27.6	15.3

Deviations from the Carman–Kozeny equation (4.9) become more pronounced in these beds of fibres as the voidage increases, because the nature of the flow changes from one of channel flow to one in which the fibres behave as a series of obstacles in an otherwise unobstructed passage. The flow pattern is also different in expanded fluidised beds and the Carman–Kozeny equation does not apply there either. As fine spherical particles move far apart in a fluidised bed, Stokes' law can be applied, whereas the Carman–Kozeny equation leads to no such limiting resistance. This problem is further discussed by CARMAN[14].

Effect of bed support. The structure of the bed, and hence K'', is markedly influenced by the nature of the support. For example, the initial condition in a filtration may affect the whole of a filter cake. Figure 4.3 shows the difference in orientation of two beds of cubical particles. The importance of the packing support should not be overlooked in considering the drop in pressure through the column since the support may itself form an important resistance, and by orientating the particles as indicated may also affect the total pressure drop.

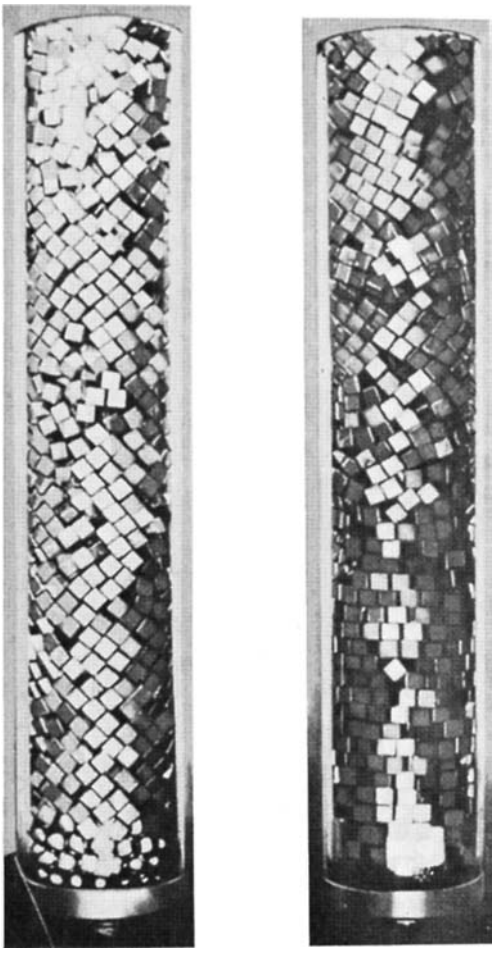

(*a*) (*b*)

Figure 4.3. Packing of cubes, stacked on (*a*) Plane surface, and (*b*) On bed of spheres

The application of Carman–Kozeny equations

Equations 4.9 and 4.16, which involve e/S_B as a measure of the effective pore diameter, are developed from a relatively sound theoretical basis and are recommended for beds of small particles when they are nearly spherical in shape. The correction factor for wall effects, given by equation 4.23, should be included where appropriate. With larger particles which will frequently be far from spherical in shape, the correlations are not so reliable. As shown in Figure 4.1, deviations can occur for rings at higher values of Re_1. Efforts to correct for non-sphericity, though frequently useful, are not universally effective, and in such cases it will often be more rewarding to use correlations, such as equation 4.19, which are based on experimental data for large packings.

Use of Carman–Kozeny equation for measurement of particle surface

The Carman–Kozeny equation relates the drop in pressure through a bed to the specific surface of the material and can therefore be used as a means of calculating S from measurements of the drop in pressure. This method is strictly only suitable for beds of uniformly packed particles and it is not a suitable method for measuring the size distribution of particles in the subsieve range. A convenient form of apparatus developed by LEA and NURSE[22] is shown diagrammatically in Figure 4.4. In this apparatus, air or another suitable gas flows through the bed contained in a cell (25 mm diameter, 87 mm deep), and the pressure drop is obtained from h_1 and the gas flowrate from h_2.

If the diameters of the particles are below about 5 μm, then *slip* will occur and this must be allowed for, as discussed by CARMAN and MALHERBE[23].

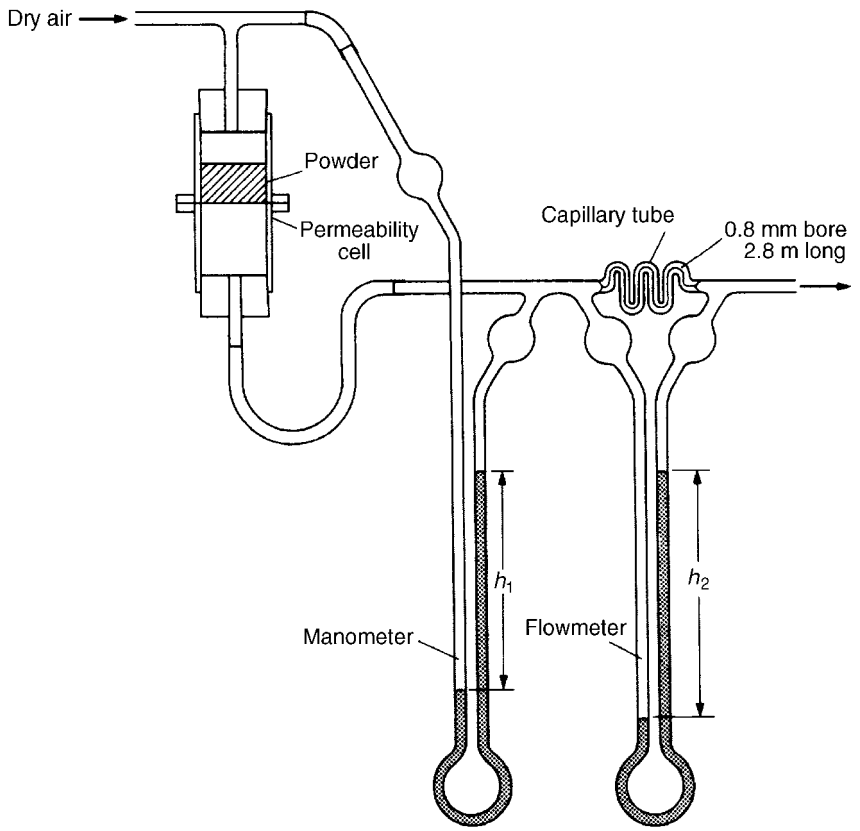

Figure 4.4. The permeability apparatus of LEA and NURSE[22]

The method has been successfully developed for measurement of the surface area of cement and for such materials as pigments, fine metal powders, pulverised coal, and fine fibres.

4.2.4. Non-Newtonian fluids

There is only a very limited amount of published work on the flow of non-Newtonian fluids through packed beds, and there are serious discrepancies between the results and conclusions of different workers. The range of voidages studied is very narrow, in most cases falling in the range $0.35 < e < 0.41$. For a detailed account of the current situation, reference should be made to work of CHHABRA *et al.*[24] and of KEMBLOWSKI *et al.*[25].

Most published work relates to the flow of shear-thinning fluids whose rheological behaviour follows the two-parameter *power-law* model (discussed in Volume 1, Chapter 3), in which the shear stress τ and shear rate $\dot{\gamma}$ are related by:

$$\tau = k\dot{\gamma}^n \tag{4.25}$$

where k is known as the consistency coefficient and n (< 1 for a shear-thinning fluid) is the power-law index.

The modelling of the flow of a non-Newtonian fluid through a packed bed follows a similar, though more complex, procedure to that adopted earlier in this chapter for the flow of a Newtonian fluid. It first involves a consideration of the flow through a cylindrical tube and then adapting this to the flow in the complex geometry existing in a packed bed. The procedure is described in detail elsewhere[24,25].

For laminar flow of a power-law fluid through a cylindrical tube, the relation between mean velocity u and pressure drop $-\Delta P$ is given by:

$$u = \left(\frac{-\Delta P}{4kl}\right)^{1/n} \frac{n}{6n+2} d_t^{(n+1)/n} \tag{4.26}$$

and the so-called Metzner and Reed Reynolds number by:

$$Re_{MR} = 8\left(\frac{n}{6n+2}\right)^n \frac{\rho u^{2-n} d_t^n}{k} \tag{4.27}$$

(Corresponding to Volume 1, equations 3.136 and 3.140)

For laminar flow of a power-law fluid through a packed bed, KEMBLOWSKI *et al.*[25] have developed an analogous Reynolds number $(Re_1)_n$, which they have used as the basis for the calculation of the pressure drop for the flow of power-law fluids:

$$(Re_1)_n = \frac{\rho u_c^{2-n}}{kS^n(1-e)^n}\left(\frac{4n}{3n+1}\right)^n \left(\frac{b\sqrt{2}}{e^2}\right)^{1-n} \tag{4.28}$$

The last term in equation 4.28 is not a simple geometric characterisation of the flow passages, as it also depends on the rheology of the fluid (n). The constant b is a function of the shape of the particles constituting the bed, having a value of about 15 for particles of spherical, or near-spherical, shapes; there are insufficient reliable data available to permit values of b to be quoted for other shapes. Substitution of $n = 1$ and of μ for k in equation 4.28 reduces it to equation 4.13, obtained earlier for Newtonian fluids.

Using this definition of the Reynolds number in place of Re_1 the value of the friction group $(R_1/\rho u_1^2)$ may be calculated from equation 4.18, developed previously

for Newtonian fluids, and hence the superficial velocity u_c for a power-law fluid may be calculated as a function of the pressure difference for values of the Reynolds number less than 2 to give:

$$u_c = \left(\frac{-\Delta P}{5kl}\right)^{1/n} \frac{1}{S^{(n+1)/n}} \frac{e^3}{(1-e)^2} \left(\frac{4n}{3n+1}\right)^{1/n} \left(\frac{b\sqrt{2}}{e^2}\right)^{(1-n)/n} \tag{4.29}$$

For Newtonian fluids ($n = 1$), equation 4.29 reduces to equation 4.9.

For polymer solutions, equation 4.29 applies only to flow through unconsolidated media since, otherwise, the pore dimensions may be of the same order of magnitude as those of the polymer molecules and additional complications, such as pore blocking and adsorption, may arise.

If the fluid has significant elastic properties, the flow may be appreciably affected because of the rapid changes in the magnitude and direction of flow as the fluid traverses the complex flow path between the particles in the granular bed, as discussed by CHHABRA[24].

4.2.5. Molecular flow

In the relations given earlier, it is assumed that the fluid can be regarded as a continuum and that there is no slip between the wall of the capillary and the fluid layers in contact with it. However, when conditions are such that the mean free path of the molecules of a gas is a significant fraction of the capillary diameter, the flowrate at a given value of the pressure gradient becomes greater than the predicted value. If the mean free path exceeds the capillary diameter, the flowrate becomes independent of the viscosity and the process is one of diffusion. Whereas these considerations apply only at very low pressures in normal tubes, in fine-pored materials the pore diameter and the mean free path may be of the same order of magnitude even at atmospheric pressure.

4.3. DISPERSION

Dispersion is the general term which is used to describe the various types of self-induced mixing processes which can occur during the flow of a fluid through a pipe or vessel. The effects of dispersion are particularly important in packed beds, though they are also present under the simple flow conditions which exist in a straight tube or pipe. Dispersion can arise from the effects of molecular diffusion or as the result of the flow pattern existing within the fluid. An important consequence of dispersion is that the flow in a packed bed reactor deviates from plug flow, with an important effect on the characteristics of the reactor.

It is of interest to consider first what is happening in pipe flow. Random molecular movement gives rise to a mixing process which can be described by Fick's law (given in Volume 1, Chapter 10). If concentration differences exist, the rate of transfer of a component is proportional to the product of the molecular diffusivity and the concentration gradient. If the fluid is in laminar flow, a parabolic velocity profile is set up over the cross-section and the fluid at the centre moves with twice the mean velocity in the pipe. This

can give rise to dispersion since elements of fluid will take different times to traverse the length of the pipe, according to their radial positions. When the fluid leaves the pipe, elements that have been within the pipe for very different periods of time will be mixed together. Thus, if the concentration of a tracer material in the fluid is suddenly changed, the effect will first be seen in the outlet stream after an interval required for the fluid at the axis to traverse the length of the pipe. Then, as time increases, the effect will be evident in the fluid issuing at progressively greater distances from the centre. Because the fluid velocity approaches zero at the pipe wall, the fluid near the wall will reflect the change over only a very long period.

If the fluid in the pipe is in turbulent flow, the effects of molecular diffusion will be supplemented by the action of the turbulent eddies, and a much higher rate of transfer of material will occur within the fluid. Because the turbulent eddies also give rise to momentum transfer, the velocity profile is much flatter and the dispersion due to the effects of the different velocities of the fluid elements will be correspondingly less.

In a packed bed, the effects of dispersion will generally be greater than in a straight tube. The fluid is flowing successively through constrictions in the flow channels and then through broader passages or cells. Radial mixing readily takes place in the cells because the fluid enters them with an excess of kinetic energy, much of which is converted into rotational motion within the cells. Furthermore, the velocity profile is continuously changing within the fluid as it proceeds through the bed. Wall effects can be important in a packed bed because the bed voidage will be higher near the wall and flow will occur preferentially in that region.

At low rates of flow the effects of molecular diffusion predominate and cell mixing contributes relatively little to the dispersion. At high rates, on the other hand, a realistic model is presented by considering the bed to consist of a series of mixing cells, the dimension of each of which is of the same order as the size of the particles forming the bed. Whatever the mechanism, however, the rate of dispersion can be conveniently described by means of a dispersion coefficient. The process is generally anisotropic, except at very low flowrates; that is the dispersion rate is different in the longitudinal and radial directions, and therefore separate dispersion coefficients D_L and D_R are generally used to represent the behaviour in the two directions. The process is normally linear, with the rate of dispersion proportional to the product of the corresponding dispersion coefficient and concentration gradient. The principal factors governing dispersion in packed beds are discussed in a critical review by GUNN[26].

The differential equation for dispersion in a cylindrical bed of voidage e may be obtained by taking a material balance over an annular element of height δl, inner radius r, and outer radius $r + \delta r$ (as shown in Figure 4.5). On the basis of a dispersion model it is seen that if C is concentration of a reference material as a function of axial position l, radial position r, time t, and D_L and D_R are the axial and radial dispersion coefficients, then:

Rate of entry of reference material due to flow in axial direction:

$$= u_c(2\pi r \delta r)C$$

Corresponding efflux rate:

$$= u_c(2\pi r \delta r)\left(C + \frac{\partial C}{\partial l}\delta l\right)$$

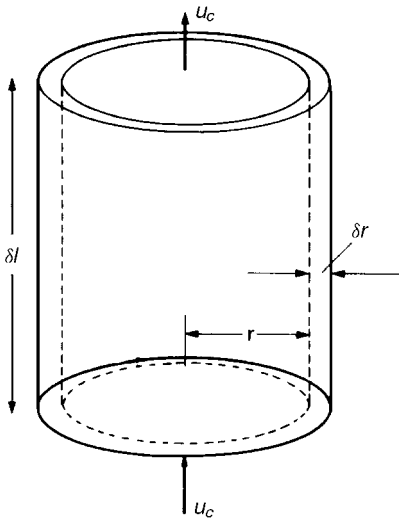

Figure 4.5. Dispersion in packed beds

Net accumulation rate in element due to flow in axial direction:

$$= -u_c(2\pi r\delta r)\frac{\partial C}{\partial l}\delta l \tag{4.30}$$

Rate of diffusion in axial direction across inlet boundary:

$$= -(2\pi r\ \delta r\ e)D_L\frac{\partial C}{\partial l}$$

Corresponding rate at outlet boundary:

$$= -(2\pi r\ \delta r\ e)D_L\left(\frac{\partial C}{\partial l} + \frac{\partial^2 C}{\partial l^2}\delta l\right)$$

Net accumulation rate due to diffusion from boundaries in axial direction:

$$= (2\pi r\ \delta r\ e)D_L\frac{\partial^2 C}{\partial l^2}\delta l \tag{4.31}$$

Diffusion in radial direction at radius r:

$$= (2\pi r\ \delta l\ e)D_R\frac{\partial C}{\partial r}$$

Corresponding rate at radius $r + \delta r$:

$$= [2\pi(r + \delta r)\ \delta l\ e]D_R\left[\frac{\partial C}{\partial r} + \frac{\partial^2 C}{\partial r^2}\delta r\right]$$

Net accumulation rate due to diffusion from boundaries in radial direction:

$$= -[2\pi r\delta l\, e]D_R\frac{\partial C}{\partial r} + [2\pi(r+\delta r)\delta l\, e]D_R\left(\frac{\partial C}{\partial r} + \frac{\partial^2 C}{\partial r^2}\delta r\right)$$

$$= 2\pi\delta l\, e\, D_R\left[\frac{\partial C}{\partial r}\delta r + r\delta r\frac{\partial^2 C}{\partial r^2} + (\delta r)^2\frac{\partial^2 C}{\partial r^2}\right]$$

$$= 2\pi\delta l\, e\, D_R\left[\delta r\frac{\partial}{\partial r}\left(r\frac{\partial C}{\partial r}\right)\right] \text{ (ignoring the last term)} \tag{4.32}$$

Now the total accumulation rate:

$$= (2\pi r\delta r\delta l)e\frac{\partial C}{\partial t} \tag{4.33}$$

Thus, from equations 4.33, 4.30, 4.31 and 4.32:

$$(2\pi r\delta r\delta l)e\frac{\partial C}{\partial t} = -u_c(2\pi r\delta r)\frac{\partial C}{\partial l}\delta l + (2\pi r\delta r e)D_L\frac{\partial^2 C}{\partial l^2}\delta l + 2\pi\delta l e D_R\left[\delta r\frac{\partial}{\partial r}\left(r\frac{\partial C}{\partial r}\right)\right]$$

On dividing through by $(2\pi r\delta r\delta l)e$:

$$\frac{\partial C}{\partial t} + \frac{1}{e}u_c\frac{\partial C}{\partial l} = D_L\frac{\partial^2 C}{\partial l^2} + \frac{1}{r}D_R\frac{\partial}{\partial r}\left(r\frac{\partial C}{\partial r}\right) \tag{4.34}$$

Longitudinal dispersion coefficients can be readily obtained by injecting a pulse of tracer into the bed in such a way that radial concentration gradients are eliminated, and measuring the change in shape of the pulse as it passes through the bed. Since $\partial C/\partial r$ is then zero, equation 4.34 becomes:

$$\frac{\partial C}{\partial t} + \frac{u_c}{e}\frac{\partial C}{\partial l} = D_L\frac{\partial^2 C}{\partial l^2} \tag{4.35}$$

Values of D_L can be calculated from the change in shape of a pulse of tracer as it passes between two locations in the bed, and a typical procedure is described by EDWARDS and RICHARDSON[27]. GUNN and PRYCE[28], on the other hand, imparted a sinusoidal variation to the concentration of tracer in the gas introduced into the bed. The results obtained by a number of workers are shown in Figure 4.6 as a Peclet number $Pe(= u_c d/eD_L)$ plotted against the particle Reynolds number $(Re'_c = u_c d\rho/\mu)$.

For gases, at low Reynolds numbers (<1), the Peclet number increases linearly with Reynolds number, giving:

$$\frac{u_c d}{eD_L} = K\frac{u_c d\rho}{\mu} = K\,Sc^{-1}\frac{u_c d}{D} \tag{4.36}$$

or:
$$\frac{D_L}{D} = \text{constant, } \gamma \text{ which has a value of approximately 0.7} \tag{4.37}$$

since Sc, the Schmidt number, is approximately constant for gases and the voidage of a randomly packed bed is usually about 0.4. This is consistent with the hypothesis that, at low Reynolds numbers, molecular diffusion predominates. The factor 0.7 is a tortuosity

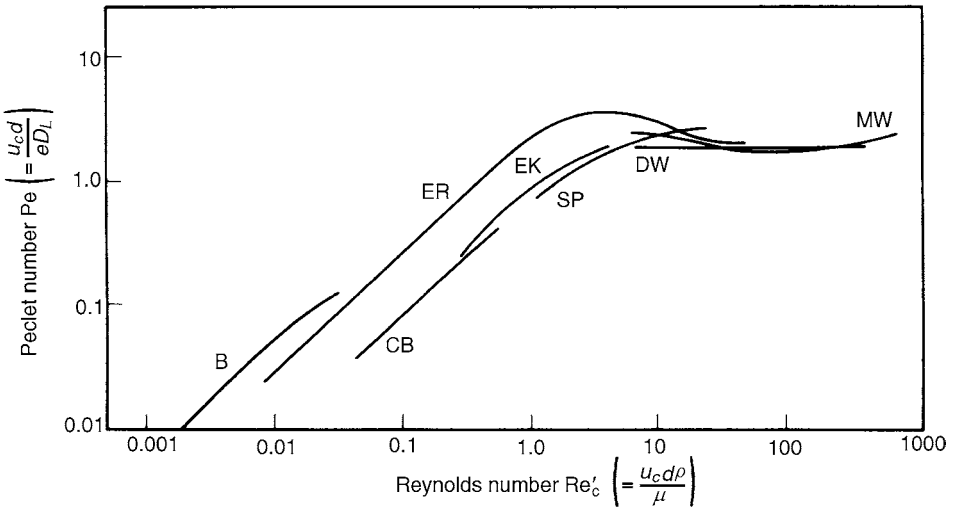

Figure 4.6. Longitudinal dispersion in gases in packed beds. ER — EDWARDS and RICHARDSON[27]; B — BLACKWELL *et al.*[29]; CB — CARBERRY and BRETTON[32]; DW — DE MARIA and WHITE[33]; MW — MCHENRY and WILHELM[34]; SP — SINCLAIR and POTTER[35]; EK — EVANS and KENNEY[36], $N_2 + He$ in $N_2 + H_2$

factor which allows for the fact that the molecules must negotiate a tortuous path because of the presence of the particles.

At Reynolds numbers greater than about 10 the Peclet number becomes approximately constant, giving:

$$D_L \approx \tfrac{1}{2}\frac{u_c}{e}d \tag{4.38}$$

This equation is predicted by the mixing cell model, and turbulence theories put forward by ARIS and AMUNDSON[30] and by PRAUSNITZ[31].

In the intermediate range of Reynolds numbers, the effects of molecular diffusivity and of macroscopic mixing are approximately additive, and the dispersion coefficient is given by an equation of the form:

$$D_L = \gamma D + \tfrac{1}{2}\frac{u_c d}{e} \tag{4.39}$$

However, the two mechanisms interact and molecular diffusion can reduce the effects of convective dispersion. This can be explained by the fact that with streamline flow in a tube molecular diffusion will tend to smooth out the concentration profile arising from the velocity distribution over the cross-section. Similarly radial dispersion can give rise to lower values of longitudinal dispersion than predicted by equation 4.39. As a result the curves of Peclet versus Reynolds number tend to pass through a maximum as shown in Figure 4.6.

A comparison of the effects of axial and radial mixing is seen in Figure 4.7, which shows results obtained by GUNN and PRYCE[28] for dispersion of argon into air. The values of D_L were obtained as indicated earlier, and D_R was determined by injecting a steady stream of tracer at the axis and measuring the radial concentration gradient across the

bed. It is seen that molecular diffusion dominates at low Reynolds numbers, with both the axial and radial dispersion coefficients D_L and D_R equal to approximately 0.7 times the molecular diffusivity. At high Reynolds numbers, however, the ratio of the longitudinal dispersion coefficient to the radial dispersion coefficient approaches a value of about 5. That is:

$$\frac{D_L}{D_R} \approx 5 \tag{4.40}$$

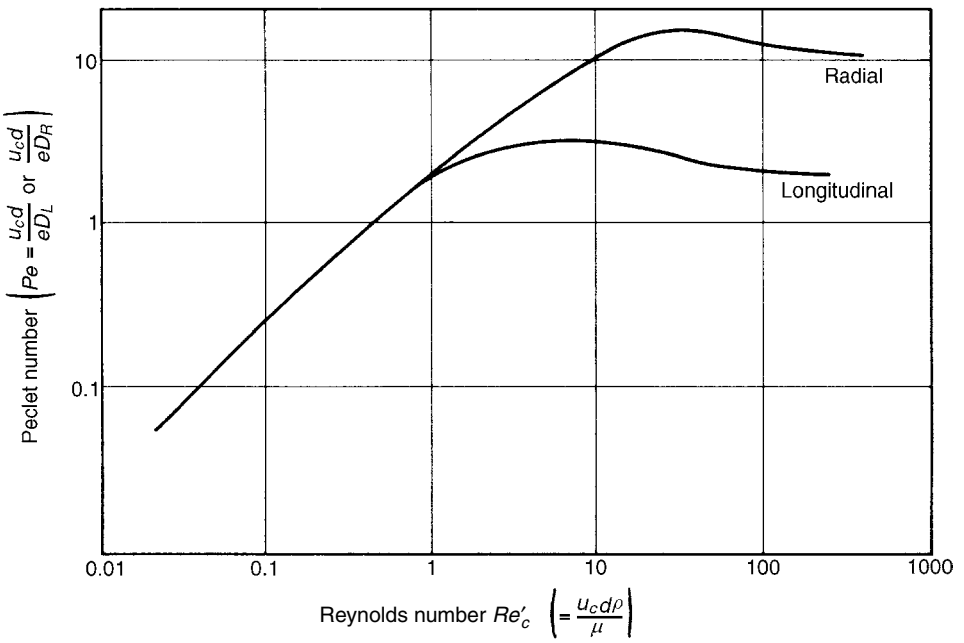

Figure 4.7. Longitudinal and radial mixing coefficients for argon in air[28]

The experimental results for dispersion coefficients in gases show that they can be satisfactorily represented as Peclet number expressed as a function of particle Reynolds number, and that similar correlations are obtained, irrespective of the gases used. However, it might be expected that the Schmidt number would be an important variable, but it is not possible to test this hypothesis with gases as the values of Schmidt number are all approximately the same and equal to about unity.

With liquids, however, the Schmidt number is variable and it is generally about three orders of magnitude greater than for a gas. Results for longitudinal dispersion available in the literature, and plotted in Figure 4.8, show that over the range of Reynolds numbers studied ($10^{-2} < Re'_c < 10^3$) the Peclet number shows little variation and is of the order of unity. Comparison of these results with the corresponding ones for gases (shown in Figure 4.6) shows that the effect of molecular diffusion in liquids is insignificant at